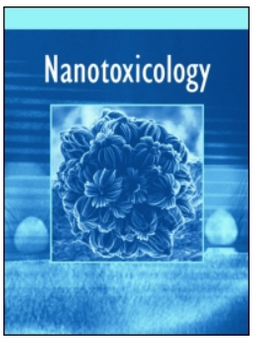

Nanotoxicology

ISSN: 1743-5390 (Print) 1743-5404 (Online) Journal homepage: http://www.tandfonline.com/loi/inan20

Probing the toxicity of nanoparticles: a unified in silico machine learning model based on perturbation theory

Riccardo Concu, Valeria V. Kleandrova, Alejandro Speck-Planche & M. Natália D. S. Cordeiro

To cite this article: Riccardo Concu, Valeria V. Kleandrova, Alejandro Speck-Planche & M. Natália D. S. Cordeiro (2017): Probing the toxicity of nanoparticles: a unified in silico machine learning model based on perturbation theory, Nanotoxicology

To link to this article: http://dx.doi.org/10.1080/17435390.2017.1379567

NANOTOXICOLOGY, 2017
https://doi.org/10.1080/17435390.2017.1379567

Taylor & Francis
Taylor & Francis Group

ORIGINAL ARTICLE

Probing the toxicity of nanoparticles: a unified *in silico* machine learning model based on perturbation theory

Riccardo Concu[a]†, Valeria V. Kleandrova[b]†, Alejandro Speck-Planche[a] and M. Natália D. S. Cordeiro[a]

[a]LAQV@REQUIMTE/Department of Chemistry and Biochemistry, Faculty of Sciences, University of Porto, Porto, Portugal; [b]Faculty of Technology and Production Management, Moscow State University of Food Production, Moscow, Russia

ABSTRACT

Nanoparticles (NPs) are part of our daily life, having a wide range of applications in engineering, physics, chemistry, and biomedicine. However, there are serious concerns regarding the harmful effects that NPs can cause to the different biological systems and their ecosystems. Toxicity testing is an essential step for assessing the potential risks of the NPs, but the experimental assays are often very expensive and usually too slow to flag the number of NPs that may cause adverse effects. *In silico* models centered on quantitative structure–activity/toxicity relationships (QSAR/QSTR) are alternative tools that have become valuable supports to risk assessment, rationalizing the search for safer NPs. In this work, we develop a unified QSTR-perturbation model based on artificial neural networks, aimed at simultaneously predicting general toxicity profiles of NPs under diverse experimental conditions. The model is derived from 54,371 NP-NP pair cases generated by applying the perturbation theory to a set of 260 unique NPs, and showed an accuracy higher than 97% in both training and validation sets. Physicochemical interpretation of the different descriptors in the model are additionally provided. The QSTR-perturbation model is then employed to predict the toxic effects of several NPs not included in the original dataset. The theoretical results obtained for this independent set are strongly consistent with the experimental evidence found in the literature, suggesting that the present QSTR-perturbation model can be viewed as a promising and reliable computational tool for probing the toxicity of NPs.

ARTICLE HISTORY
Received 17 March 2017
Revised 21 August 2017
Accepted 8 September 2017

KEYWORDS
Cytotoxicity; ecotoxicity; nanoparticles; prediction; QSTR-perturbation model

Introduction

The 21st century has witnessed the dynamic and accelerated growth of nanotechnology, an emerging discipline that has revolutionized modern science. In fact, there have been many applications of nanoparticles (NPs) in diverse areas ranging from optics, photonics (Chan et al. 2013; Schoen et al. 2013; Zhang et al. 2013), and electronics (Chen et al. 2012; Kim et al. 2013; Liz-Marzán and Kamat 2004) to magnetism (Corchero and Villaverde 2009) as well as catalytic processes in material sciences and chemistry (Biffis and Králik 2001; Chan et al. 2013; Lu et al. 2013b; Moseler et al. 2012; Yang et al. 2013), including biomedicine (Brigger et al. 2002; Liao et al. 2014; Lu et al. 2013a). However, despite the benefits that the use of NPs can bring, the massive production and manipulation of new NPs have created serious concerns regarding the possible toxic effects that can affect the biological systems (including humans) and their respective ecosystems. Therefore, the assessment of multiple toxicity profiles of NPs constitutes a goal of particular interest in order to determine the potential hazards of any nanoentity.

Powerful experimental techniques involving high throughput/content screening (HTS/HCS) may play an important role for the evaluation of the toxicity of the NPs (Holden et al. 2013). However, obtaining evidence from such bioassays is often expensive and time-consuming. In the particular case of NPs, this stems from the fact that they embody a huge chemical diversity, range of types, sizes, shapes, etc., clearly associated to a wide spectrum of different biological behaviors. Thus, it is almost impossible to

CONTACT Alejandro Speck-Planche alejspivanovich@gmail.com LAQV@REQUIMTE/Department of Chemistry and Biochemistry, Faculty of Sciences, University of Porto, Porto 4169-007, Portugal; M. Natália D. S. Cordeiro ncordeir@fc.up.pt LAQV@REQUIMTE/Department of Chemistry and Biochemistry, Faculty of Sciences, University of Porto, Porto 4169-007, Portugal
†Authors contributed equally.

Supplemental data for this article can be accessed here.

cover and filter the chemico-biological space with the use of experimental techniques, and above all, impracticable to cope with the booming of nano-enabled consumer products introduced on the market.

One way to alleviate the above problems is to apply computational methods that may well aid in both the prioritization and risk assessment of NPs. Among them, quantitative-structure activity/toxicity relationships (QSAR/QSTR) models have been very useful for the virtual prediction of toxicities of NPs, helping to rationalize the search for safer nanomaterials, and providing the foundations regarding the essential aspects responsible for unshackling the toxic effects (Fourches et al. 2010; Liu et al. 2011; Liu et al. 2013; Puzyn et al. 2011; Epa et al. 2012; Toropov et al. 2012; Shao et al. 2013; Kar et al. 2014). Nevertheless, most of the current QSAR/QSTR models have been based on classical concepts and generaly have resorted to linear analyses. That is, they have attempted to predict the toxicity of the NPs against only one biological system (*e.g.* cell line, crustacean, alga, bacterium, fungus, plant, fish, etc.), and usually the NPs chemical composition and size being the only factors considered. At the same time, these models do not disclose any information concerning the influence of key biological and/or physicochemical factors, such as the different kinds of measures of toxicity (including ecotoxicity and cytotoxicity), the shape of the NPs, the media under which the sizes of the NPs have been determined, and the times of the assays, *i.e.* the intervals of time during which the diverse biological systems have been exposed to the NPs. Here, it should be emphasized that the *in silico* evaluation of the NPs' toxicity might be a very difficult task whenever large databases (several hundreds of NPs) are used.

Very recently, a promising perturbation-based approach of wide applicability has been established, and the derived *in silico* models have been rigorously validated. The latter in turn were shown to be able of reliably predicting different biological and/or physicochemical properties under many experimental conditions (Gonzalez-Diaz et al. 2013). Indeed, this approach has already been successfully applied for the prediction of diverse toxicity profiles of NPs subjected to dissimilar assays conditions (Kleandrova et al. 2014a, 2014b; Luan et al. 2014). Despite the great importance of the latter works, only linear relationships between the physicochemical factors and the toxic effects have been attempted. Nevertheless, the nature behind the interaction of NPs with biological systems is very complex, and thus, more complex data analysis methods are needed. This work thus aims at developing a novel QSTR-perturbation model for jointly predicting multiple toxicological profiles of NPs under diverse experimental conditions, but based on one of such non-linear analysis methods, namely on artificial neural networks (ANN).

Materials and methods

Dataset

The dataset employed to generate the model was collected from different sources published in the literature (Ha et al. 2014; Hussain et al. 2005; Salunkhe et al. 2013; Radziun et al. 2011; Gonzalez et al. 2010; Jeng and Swanson 2006; Li et al. 2012; Uboldi et al. 2012; Lin et al. 2006; Chusuei et al. 2013; Song et al. 2014; Horev-Azaria et al. 2013; Carlson et al. 2008; Ahamed et al. 2013; Motskin et al. 2009; Selvaraj et al. 2014; Saquib et al. 2013; Ahamed et al. 2010; Coradeghini et al. 2013; Grosse et al. 2013; Fraga et al. 2013; Xu et al. 2012; Wang et al. 2012; Ahamed 2011; Sabbioni et al. 2014; Bhattacharjee et al. 2013; Tarantola et al. 2011; Chueh et al. 2014; Heinlaan et al. 2008; Mortimer et al. 2010; Hund-Rinke and Simon 2006; Sadiq et al. 2011a; Gong et al. 2011; Griffitt et al. 2008; Sadiq et al. 2011b; Tuominen et al. 2013; García et al. 2011; Franklin et al. 2007; Han et al. 2012, Ma et al. 2010; Lin and Xing 2007; Ma et al. 2011; Zhu et al. 2009; Zhu et al. 2010; Pakrashi et al. 2013; Wang et al. 2009, Asharani et al. 2011; Bar-Ilan et al. 2009; Zhu et al. 2008; Zhang et al. 2012, Silva et al. 2014; Marsalek et al. 2012; Nations et al. 2011; Artells et al. 2013, Yang et al. 2010; Truong et al. 2011; Zanette et al. 2011; Cho et al. 2013; Song et al. 2013; Chen et al. 2013, Kwon et al. 2014; Liang et al. 2014; Sadeghi et al. 2015; Kasemets et al. 2009). In so doing, we were able to compile a set of 260 unique NPs with 31 chemical compositions, ranging from solely metal-based to metallic oxide NPs, including silica-based NPs. For these NPs, we gathered results pertaining to ecotoxity or/and cytotoxicity assays. The data then embody at least 1 out of the 5 reported types of toxicity measures

(m_e), specifically: the cytotoxic concentration of the NPs causing 50% reduction in cell viability [CC_{50} (μM)], the effective concentration of the NPs inducing a response halfway between the baseline and maximum after a specified exposure time of a biological system [EC_{50} (μM)], the concentration of the NPs that prevented the root elongation of the plant at 50% [IC_{50} (μM)p], and the concentrations causing toxic [TC_{50} (μM)] and lethal [LC_{50} (μM)] effects in 50% of the biological systems. Since the latter toxicity assays targeted different endpoints – for instance: algae, bacteria, fungi, mammal cell lines, crustaceans, plants, fishes, among others, the data further include at least 1 out of those 53 different endpoints (b_t). Additionally, we took into account that for the same NPs, at least 1 out of 11 categories of shape (n_s) have been reported, their sizes have been determined in at least 1 out of 8 conditions (d_m), and at least 1 out of 16 different assay times (t_a) employed; the latter ranging from 0.5 to 360 hrs. Moreover, it should be noticed that 194 NPs have been tested in their pure uncoated form but not the remaining 66, on which at least 1 out of 16 organic molecules have been used as surface coating agents (s_c). All this data's information is specified in file SM1 of the Supporting Information (SI), including a detailed list of the 260 NPs, the kind of biological systems, cell lines, plants and fishes exposed to them, if they are coated or not, their sizes and shapes, the reported exposition times, along with the corresponding papers from which such information was retrieved.

From now on, to systematize whole the collected data we will use the terminology 'experimental conditions,' expressed as an ontology of the form $c_j \rightarrow (m_e, b_t, n_s, d_m, t_a, s_c)$. Like this, the variation of at least one of the elements of c_j *via* its different categories or labels will always represent a *unique* experimental condition. One should notice also that, the use of the ontology c_j permits a greater degree of customization for each toxicity assay, providing a more efficient control of the uncertainty of the experimental data.

Finally, the original 260 NPs were clustered into two groups, so-called 'nontoxic' and 'toxic.' A NP was assigned to the group of nontoxic [TE_i (c_j) = 1] if its toxicity satisfied at least one of the following criteria: CC_{50} (μM) ≥ 188.57, EC_{50} (μM) ≥ 168.46, IC_{50} (μM)$p \geq 245.68$, TC_{50} (μM) ≥ 126.52, or LC_{50} (μM) ≥ 250. Otherwise, the NP was chosen as toxic [TE_i (c_j) = −1]. Notice here that $TE_i(c_j)$ is a binary categorical variable that allows the classification between the two groups of NPs according to their values of toxicities. In addition, two main reasons driven the adoption of such criteria, *i.e.* Firstly, NPs are typically employed in a range higher than μM. Due to this, and in accordance with the works from which the data were collected, the thresholds were selected high enough to ensure that if a NP is predicted as nontoxic it will really have no toxic effects. The second reason was due to the fact that those thresholds led to a reasonably well-balanced ratio of nontoxic/toxic NPs in the dataset.

Molecular descriptors

Two families of molecular descriptors were used in this work for tackling the nanoparticles *per se*. From one side, four descriptors related to their physicochemical properties were considered, *i.e.* the molar volume (V), electronegativity (E), polarizability (P), and the size of the NPs (L). The first three properties were retrieved from the public source known as Chemicool Periodic Table (Hsu 2013) and in the case of NPs with two or more different atoms, these were averaged over the constituting atoms. The values of the fourth one were gathered from available experimental data. The other family of descriptors considered were 2D-topological descriptors, the well-known spectral moments of the bond adjacency matrix. Basically, these graph-based molecular descriptors were computed with the MODESLAB software (Estrada and Gutiérrez 2002–2004) from inputting the SMILES codes generated for the NPs. Specifically, we have computed spectral moments from order 0 to 3 [$\mu_k(PP)$, $k = 0, 1, 2, 3$], and the latter three ($k = 1$–3) being weighted by the following atomic properties: polarizability (POL), van der Waals atomic radius (VAN), and atomic weight (ATO); μ_0 stands for the number of bonds in the NPs.

In what regards, the descriptors used for undertaking the coating agents of the nanoparticles, these were calculated as follows:

$$G\mu_k(PP)s_c = \mu_k(PP)s_c \cdot \sqrt[2]{NMU} \quad (1)$$

In this equation, $\mu_k(PP)s_c$ refer also to spectral moments of the bond adjacency matrix but with k

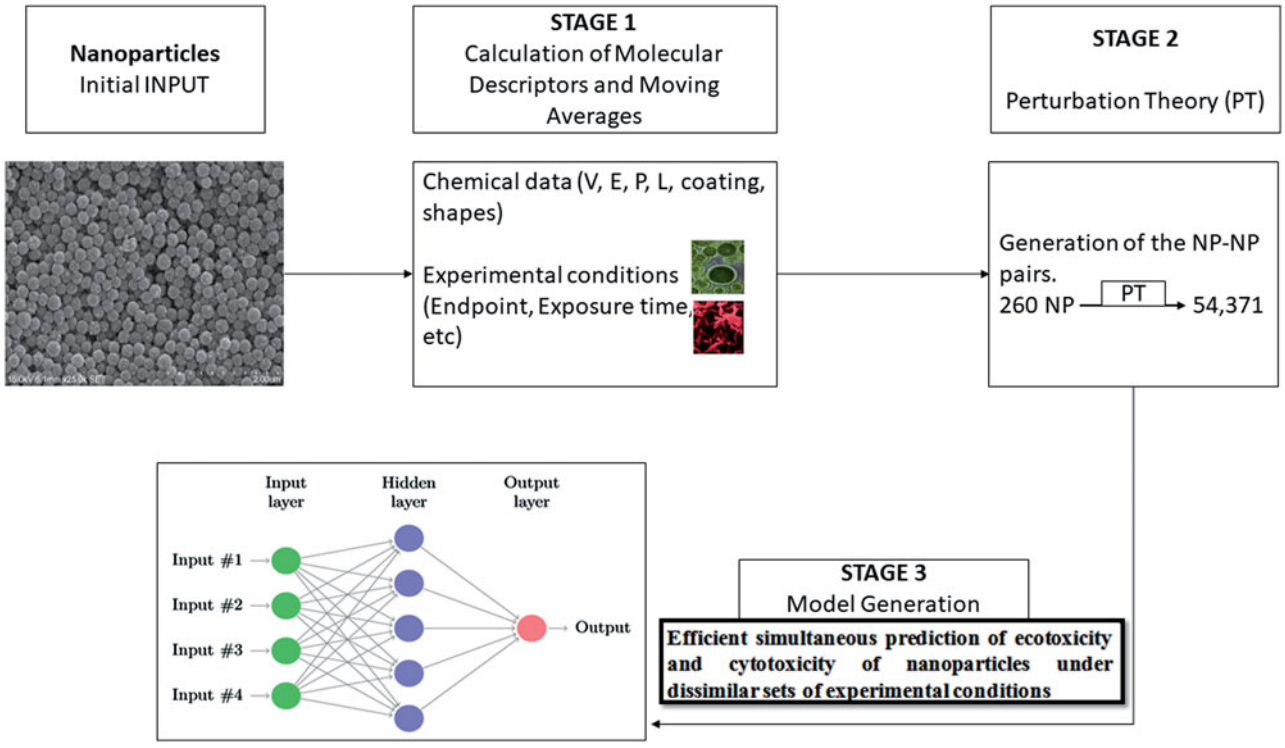

Figure 1. Main stages involved in the setting-up of the QSTR-perturbation model based on ANN.

ranging from 0 to 5 (μ_0 stands for the number of bonds in the caoating agents, excluding the hydrogen atoms), and the latter five ($k = 1$–5) being weighted by hydrophobicity (HYD) and polar surface area (PSA); these descriptors were calculated using the same software as referred to above. The symbol *NMU* represents the number of monomeric units, its value being 1 for single organic molecules. For the case of a polymer, *NMU* was defined as the quotient between the molecular weight of the polymer and the molecular weight of the monomer (or sum of monomers if more than one). Finally, the symbol $G\mu_k(PP)s_c$ stands for the generalized spectral moments of the bond adjacency matrix and naturally, we have considered $G\mu_k(PP)s_c = 0$ for uncoated NPs.

QSTR-perturbation model set-up and evaluation

A three-stage procedure was followed for setting-up the QSTR model, according to the perturbation theory-based approach (Gonzalez-Diaz et al. 2013) (Figure 1).

To begin with, since the descriptors previously mentioned above are not able to discriminate the toxicological profiles of the NPs when any element of the ontology c_j is modified, a new set of descriptors were defined by applying the moving average approach (Hill and Lewicki 2006):

$$DX_i(c_j) = X_i - avgX_i(c_j) \quad (2)$$

In Equation (2), X_i stands for the different descriptors describing the various NPs [*V*, *E*, *P*, *L*, and $\mu_k(PP)$], whereas $avgX_i(c_j)$ means the average of the X_i values for all the NPs tested against the same element of c_j. For example, in the case of a defined biological system b_t – cell line, fish, crustacean, etc., $avgX_i(c_j)$ was obtained as the average of the X_i values for all the NPs tested against that specific biological system. The same procedure was followed up for the other elements of the ontology c_j. In any case, we only used the descriptors of the type $DX_i(c_j)$ because they involved both the molecular entities/chemical compositions associated to the NPs and the ontology c_j. All information related to the NPs and coating agents used, retrieved experimental data for these, their classification group, along with the applied $DX_i(c_j)$ and $avgX_i(c_j)$ descriptors is shown in file SM2 of SI.

The second stage is aimed at overcoming another limitation of the current classical QSTR linear models used for NPs (Fourches et al. 2010; Liu et al. 2011; Liu et al. 2013; Puzyn et al. 2011; Epa et al. 2012; Toropov et al. 2012; Shao et al. 2013;

Kar et al. 2014). Notice that in these classical models, the intercept of the model linear equation is often interpreted as the magnitude of the targeted endpoint (toxicity) for a hypothetical reference chemical. This is, however, a major limitation since any chemical entity in a dataset may be used as reference. The perturbation theory approach attempts to solve such limitation by introducing the concept of case-case pairs, which are defined by making combinations of the dataset original cases. In each of these pairs, one of the cases is taken as the reference state (*rf*) while the other as the new or output state (*nw*) to be predicted. Therefore, a specific case can be predicted (new state) from all the other cases, and at the same time, that case can participate as reference state to predict the others. This strategy allows in turn to find possible deviations (or perturbations) among the defined pairs due to differences related to their chemical composition and ontology' elements.

Herewith, the 260 original NP cases were uniformly randomly combined to produce a total of 54,371 pairs (*i.e.* ~80% of all possible pairs). As described above, in each pair, one of the NPs along with all its data was used as reference state whereas the other (also together with all its data) was used as the new state. Then, the differences between the NP pairs were calculated using the following expression:

$$DDX_i(c_j) = DX_i(c_j)_{\_nw} - DX_i(c_j)_{\_rf} \quad (3)$$

In this equation, $DX_i(c_j)_{\_nw}$ and $DX_i(c_j)_{\_rf}$ are the same as the set of descriptors depicted in Equation (2), but the symbols have been adapted to represent the descriptors of the NPs in the new and reference states, respectively. A similar expression was applied to account for the differences in the structures of the coating agents of the NP pairs, that is:

$$DG\mu_k(PP)s_c = G\mu_k(PP)s_{c\_nw} - G\mu_k(PP)s_{c\_rf} \quad (4)$$

where $G\mu_k(PP)s_{c\_nw}$ and $G\mu_k(PP)s_{c\_rf}$ represent the descriptors of the coating agents for the NPs in the new and final states, respectively. From Equations (3) and (4), one can easily grasp that the descriptors $DDX_i(c_j)$ and $DG\mu_k(PP)s_c$ can be viewed as perturbation terms.

Finally, the third stage is focused on establishing the general expression to predict the toxicity of the NPs under diverse experimental conditions. This proceeds as follows: The generated dataset containing the 54,371 pairs was randomly split into two series, *i.e.* training and validation sets. The training set was used to find the QSTR-perturbation model, and comprised 40,804 cases, being 26,131 nontoxic and 14,673 toxic. The validation set was employed to analyze the predictive power of the model. This set had 13,567 cases, with 8613 nontoxic and 4954 toxic. Here, one should to point out that each of theses cases is a NP-NP pair and consequently, the terms 'nontoxic' and 'toxic' refer to the NPs to be predicted, *i.e.* to the NPs in the new states. We are now in position of setting up the QSTR-perturbation model using the following general expression:

$$TE_i(c_j)_{\_nw} = f[TE_i(c_j)_{\_rf}, DDX_i(c_j), DG\mu_k(PP)s_c] \quad (5)$$

The meaning of Equation (5) is that the toxic effect of any NP in the new state $[TE_i(c_j)_{\_nw}]$ is a function (f) that depends on the toxic effect of the NP used in the reference state $[TE_i(c_j)_{\_rf}]$, and the perturbation terms $DDX_i(c_j)$ and $DG\mu_k(PP)s_c$. Notice also that $TE_i(c_j)_{\_nw}$ and $TE_i(c_j)_{\_rf}$ are binary/categorical variables with exactly the same meaning as $TE_i(c_j)$, which was previously described. Additionally, due to the complexity of modeling the toxicity of NPs, f is a non-linear function with high degree of complexity. In the specific case of the present study, f was found by employing the data analysis method ANN, and by resorting to the ANN module named Intelligent Problem Solver implemented in the STATISTICA® package (Statsoft-Team 2001).

To begin with, different ANN architectures and topologies were investigated such as linear neural network (LNN), radial basis function (RBF), multilayer perceptron (MLP), and probabilistic neural network (PNN). As to the topology of any neural network, given the commonly empirical knowledge, the number of neurons in the hidden layer should be between the number of neurons in the input layer and the number of neurons in the ouput layer. However, this rule does not hold due to very simple reasons. Firstly, the rule does not consider aspects such as the complexity of the phenomenon under study, or the number of training samples, and both of them are crucial for the development of a model based on ANN. It has been reported that the number of neurons in the hidden layer can be higher than the sum of neurons in the input and output layers (Stathakis 2009). In fact, it has been

mathematically proven that standard single-hidden layer feedforward networks (MLP belongs to this group) with at most N hidden neurons (including biases) can learn N distinct samples with zero error, and this is applicable to any non-linear activation function (Huang and Babri 1998). However, the only agreement between the aforementioned empirical knowledge and the mathematical evidence is that the number of neurons in the hidden layer should be as low as possible. The present QSTR-perturbation model was built up from a training set containing $N = 40{,}804$ pair cases, and the best model found had the following ANN profile: MLP 10:10-44-1:1. This means that the derived ANN model used 10 descriptor variables from which 10 neurons were generated in the first layer, the second (hidden) layer contained 44 neurons, while the output layer had one neuron that allowed predicting the response variable $[TE_i(c_j)\_{nw}]$. If one takes into account the great complexity of predicting the toxic effects of NPs under multiple experimental conditions, one might think that only 44 neurons to correlate 40,804 inputs implies underfitting. However, the following strategy was adopted by us to prevent both underfitting and/or overfitting problems. Initially, we ran a large set of 50 different ANN models with the Intelligent Problem Solver included in the STATISTICA® package in order to identify the best network architecture and topology for our dataset. After this first step, we find out that the best architecture for our problem was MLP. Due to this, we ran another set of 50 ANN models in order to identify the MLP topology that best fitted our dataset. From those runs, it was evident that the best topology models were obtained using a number of neurons around 44, in fact we could not find any better model even increasing the number of neurons in the hidden layer up to 50.

Furthermore, a sensitivity analysis was carried out with the aim of identifying and selecting the most significant descriptors to be included in the QSTR-perturbation model. Sensitivity analysis in data mining and statistical model building/fitting generally refers to the assessment of the importance of the descriptor variables in the model. In short, given a fitted model with certain parameters, it discloses what is the effect of varying the parameters of the model (for each descriptor variable) on the overall model fit properties. To do so, the aforementioned ANN module computes the sum of squares residuals or misclassification rates for the model when a descriptor variable is eliminated from the neural net. Therefore, the descriptor variables can be sorted by their importance or relevance for the particular neural net. Moreover, in such ANN module, only descriptors with values of sensitivity higher than one are considered. Another important detail is that, as usual, inter-correlations between the descriptor variables were determined in order to diminish any possible negative effects in the performance of the model.

Finally, the statistical quality (training set) and predictive power (validation set) of the QSTR-perturbation model based on ANN were assessed by considering diverse statistical indices. These included, for example, the percentages of correct classifications for nontoxic (sensitivity – SENS) and toxic (specificity – SPEC) cases, the overall percentage of correct classifications (accuracy), the Matthews correlation coefficient (MCC) (González-Díaz et al. 2007), and the areas under the receiver operating characteristic (ROC) curves (Hanczar et al. 2010).

Results and Discussion

QSTR-perturbation ANN-based model

As referred above, the derived model has the following ANN profile: MLP 10:10-44-1:1. The symbols of the ten employed descriptor variables along with their definitions are shown in Table 1.

This ANN model was found to correctly classify 25,791 out of 26,131 nontoxic cases (SENS = 98.7%) and 14,414 out of 14,673 toxic cases (SPEC = 98.2%) in the training set, leading to an overall accuracy of 98.5%. As regards the validation set, 8468 out of 8613 nontoxic cases (SENS = 98.3%) and 4848 out of 4954 toxic cases (SPEC = 97.86%) were properly predicted, affording an overall accuracy of 98.2%. Additionally, the obtained MCC values were 0.968 and 0.960 for the training and validation sets, respectively. These values are very close to 1, thereby confirming the very strong correlation between the observed and predicted values of the categorical variable of toxicity $[TE_i(c_j)\_{nw}]$. In what concerns, the determined ROC curves (Figure 2), the areas obtained under these curves were 0.999 and 0.998 for the training and validation sets, respectively. These values indicate that the derived ANN

Table 1. Descriptors used on the present QSTR-perturbation model.

Descriptor	Concept
$TEi(c_j)\_{rf}$	Dummy classification variable describing the toxic effect of the NP used in the reference state.
$DDV(m_e)$	Perturbation term that characterizes the change of the molar volume between the NPs used in the new output and reference states, also depending on the measures of the toxic effects.
$DDL(m_e)$	Perturbation term that accounts for the variation of the size between the NPs used in the new and reference states, also depending on the measures of the toxic effects.
$DD\mu_1(ATO)b_t$	Perturbation term that describes the difference of the spectral moment of order 1 (weighted by the atomic weight) between the NPs used in the new and reference states, also depending on the biological systems.
$DD\mu_3(POL)n_s$	Perturbation term that characterizes the change of the spectral moment of order 3 (weighted by the polarizability) between the NPs used in the new and reference states, also depending on the shapes of the NPs.
$DDE(d_m)$	Perturbation term that describes the variation of the electronegativity between the NPs used in the new and reference states, also depending on the conditions under which the sizes of the NPs were measured.
$DD\mu_3(VAN)t_a$	Perturbation term that accounts for the difference of the spectral moment of order 3 (weighted by the atomic van der Waals radius) between the NPs used in the new and reference states, also depending on the exposure times.
$DD\mu_2(ATO)_{ta}$	Perturbation term that characterizes the change of the spectral moment of order 2 (weighted by the atomic weight) between the NPs used in the new and reference states, also depending on the exposure times.
$DG\mu_2(Hyd)s_c$	Perturbation general spectral moment of order 2 weighted by the hydrophobicity, which accounts for the difference between the chemical structures of the coating agents used in the new and reference states.
$DG\mu_5(PSA)s_c$	Perturbation general spectral moment of order 5 weighted by the polar surface area, which characterizes the difference between the chemical structures of the coating agents used in the new and reference states.

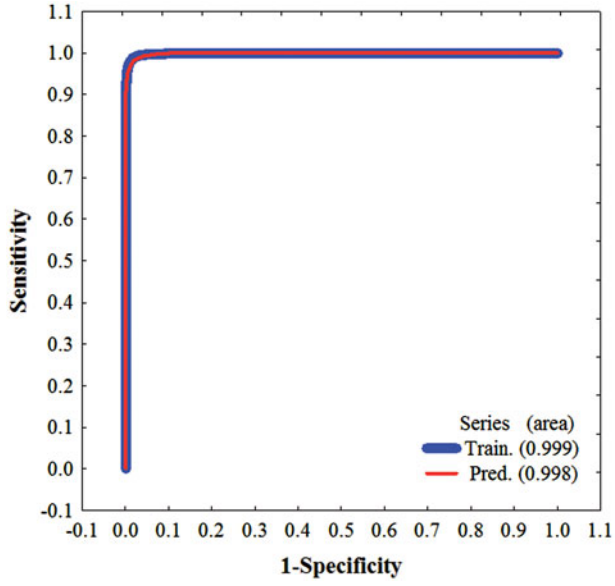

Figure 2. ROC curves for the training and validation sets used.

model does not behave as a random classifier because the areas are very different from a model that performs random classifications (area = 0.5). The closeness to 1 for the areas under the ROC curves also suggests the model is able to perform very accurate predictions.

As a final validation tool, we have applied the Y-randomization approach (Rücker et al. 2007) to check the robustness of the present ANN model in data description. To do so, the SENS and SPEC statistical indices of our original model were compared to those obtained from models built for ten permuted (randomly shuffled) responses, leaving the set of reference states intact (see Table 2). Specifically, 10 models were built based on the original descriptor pool and the original model building procedure (MLP 10:10-44-1:1). As can be seen, all these models led to values of SENS ranging from 0% to 98.6%, and of SENS ranging from 1% to 100% (overall accuracy between 59.5% and 64.0%), that is, values far worse than the ones found with our original ANN model. These results are typical of random models thus, further assuring robustness and statistical significance of our models.

To sum up, all the statistical results demonstrate that the present QSTR-perturbation ANN-based model displays an excellent performance in modeling the toxicological profiles of NPs under different experimental conditions. Although its performance is similar to the one attained with other models previously reported (Kleandrova et al. 2014a, 2014b; Luan et al. 2014), the present QSTR-perturbation model predicts more statistical cases of NPs, that is, many more experimental conditions regarding the ecotoxicity and cytotoxicity of NPs are considered here. In addition, the influence of the use of coating agents is evaluated, taking into account the number and meaning of the descriptors of these organic molecules on the surface of the NPs. The results of the classification for each NP-NP pairs, as well as all the relevant toxicological, chemical data, and statistical data can be found in SI (files SM3–SM6). The neural network file is also provided in SI (file SM7).

Influence of the descriptors in the toxicity profiles of the NPs

The next step is to find out the most significant factors that can affect the toxicological profiles of the

Table 2. The SENS and SPEC values of ten Y-randomization tests.

No.	SENS (%)[a]	SPEC (%)[a]	Accuracy (%)[b]
1	93.5	6.70	62.3
2	0.00	100.	64.0
3	0.03	100.	64.0
4	0.00	100.	64.0
5	0.48	99.5	63.9
6	0.63	99.4	63.9
7	82.7	17.3	59.5
8	97.8	2.18	63.4
9	88.6	11.4	60.9
10	98.6	1.40	63.6

[a]Percentages of correct classifications for non-toxic cases (SENS) and for toxic cases (SPEC).
[b]Accuracy, *i.e.* overall percentage of correct classifications.

different NPs. This can be examined since each descriptor/perturbation term that entered in the model contains information regarding the chemical composition of the NPs, and at the same time, it depends on at least one of the elements of the experimental conditions/ontology c_j. For interpretation of the results, we will focus on on the most significant descriptors that influence the NPs toxicity by calculating their sensitivities. A larger value of sensitivity will be always associated to a higher degree of influence of the descriptor in the ANN QSTR-perturbation model.

It is well-known that models based on non-linear ANN do not lead to simply equations as they embrace very complex functions. Therefore, it is difficult to understand how the variations of the included descriptors will be responsible for triggering the changes in the toxicities of any chemical species. Despite the lack of equations, we can try to interpret the changes of the diverse descriptors in such kinds of ANN-based models following a simple approach (Speck-Planche and Kleandrova 2012). If the average values of the descriptors/perturbation terms for nontoxic and toxic cases are compared between each other, then, it is possible to have an idea regarding the tendency of the variation of the descriptors/perturbation terms in the model. In other words, comparing the average values of the descriptors for nontoxic and toxic cases with the specific value of the descriptor of each toxic or nontoxic input, we can have an idea wether the compound is likely to be toxic or not. This further prompt us to analyze how the physicochemical properties associated to the descriptors/perturbation terms may undergo variations in order to decrease the toxicity of the NPs to be predicted (new states). Such analysis will be based on the data shown in Table 3, which contains values of the sensitivities of all the descriptors, as well as of the average values for the perturbation terms of nontoxic and toxic cases.

Let us start by the descriptor $TE_i(c_j)\_rf$ (eighth in the ranking; see Table 3), which characterizes any NP used as reference from which other NPs are to be predicted (new output states). Notice that the perturbation approach was applied in such a way that the NP-NP pairs were obtained by mixing different NP cases belonging to any of the groups of classification (nontoxic and toxic). An inspection of the values of $TE_i(c_j)\_rf$ and $TE_i(c_j)\_nw$ for each NP-NP pairs (files SM5 and SM6 of SI), combined with the high percentages of correct classifications (SENS, SPEC, and accuracy), lead us thus to deduce that the developed QSTR-perturbation model based on ANN can tackle both similarity and dissimilarity of the NPs in terms of their toxicities.

From a close analysis of the values in Table 3, one can see that the decrease of the toxicity of the NPs can be influenced by the increment of the molar volume, which is characterized by the perturbation term $DDV(m_e)$. This important descriptor (the fourth most significant) describes the variations in the chemical compositions between any two NPs, depending also on the measures of the toxicities. The increment of the molar volume is directly proportional with the increment (but is not only limited to) the number of metallic atoms. Notice that by definition, the molar volume is the volume occupied by a mole of substance, chemical element, or compound. Therefore, the molar volume expresses in some way the tendency of the substance to experience agglomeration or aggregation. Additionally, due to its direct correlation with the molar mass, NPs with compositions containing heavier atoms will have larger molar volumes. Such NPs will have more tendency to aggregate or agglomerate, and so leading to an increase of their size that is a favorable factor in the diminution of the toxic effects. Related also with agglomeration/aggregation processes, the increment of the sizes of the NPs will diminish their toxicities. This comes from the fact that NPs with larger sizes will not be able to penetrate through different biological membranes, and then, the biological systems will not suffer remarkable damage. The increment in the sizes of the NPs is accounted for by $DDL(m_e)$

Table 3. Sensitivities and mean values of the different descriptors.[a]

Descriptor	Sensitivity	Average (nontoxic)	Average (toxic)	Tendency
$TE_i(c_j)\_rf$	6.570	–	–	–
$DDV(m_e)$	9.075	0.280	−0.355	Increase
$DDL(m_e)$	7.724	6.613	−11.588	Increase
$DD\mu_1(ATO)b_t$	8.939	−0.209	−0.383	Increase
$DD\mu_3(POL)n_s$	4.572	12.058	−13.577	Increase
$DDE(d_m)$	16.702	0.193	−0.320	Increase
$DD\mu_3(VAN)t_a$	10.504	11.544	−15.314	Increase
$DD\mu_2(ATO)t_a$	6.473	−279.465	369.089	Decrease
$DG\mu_2(HYD)s_c$	8.299	−1.664	14.729	Decrease
$DG\mu_5(PSA)s_c$	16.139	3442785.757	1604305.543	Increase

[a]All data are referred to the training set.

(seventh in the raking), which depends on the changes in the chemical compositions between any two NPs, and on the measures of the toxicities. The joint analysis of the perturbation terms $DDV(m_e)$ and $DDL(m_e)$, allow us to confirm that the toxicities of the NPs are concentration/assay-dependent. The descriptor with the higher degree of importance (first in the ranking) in the QSTR-perturbation model based on ANN is $\Delta\Delta E(d_m)$, and it embodies the difference of electronegativity between any two NPs, depending also on the conditions (media) under which the sizes of the NPs were determined. Thus, the general tendency associated with the incorporation of electronegative atoms to the molecular compositions of the NPs (preferably O, S) will increase the value of $\Delta\Delta E(d_m)$, with the subsequent decrease of their toxic effects.

On the other hand, Table 3 provides the information regarding the influence of the descriptors/perturbation terms of the type $DD\mu_k(PP)c_j$ (see the symbols associated to Equation (3) and files SM5 and SM6 in SI). These are very important because they can differentiate NPs containing metallic cores from those containing more than one atom corresponding to more than one chemical element. Indeed, the variation of any $DD\mu_k(PP)c_j$ perturbation term can be beneficial for NPs formed by more than one different atom, and at the same time, the variation can be detrimental for metallic NPs. Notice that these $DD\mu_k(PP)c_j$ perturbation terms will always be equal to zero for metallic NPs, and different from zero, otherwise. The order k of these perturbation terms gives an idea about which kinds of molecular structures forming the NPs are more desirable for the diminution of their toxic effects.

Starting with the $DD\mu_1(ATO)b_t$, one can infer that its increment will cause a diminution in the toxic effects of the NPs due to the increase in the global molecular weight/molar mass. This descriptor/perturbation term is among the most significant (fifth in the ranking) in the QSTR-perturbation model based on ANN because it considers the variations of the physicochemical property mentioned above between any pair of NPs, depending also on the biological systems against which the NPs were tested. Nevertheless, $DD\mu_1(ATO)b_t$ is constrained by $DD\mu_2(ATO)t_a$ (penultimate descriptor in terms of importance), which characterizes the decrease of the same physicochemical property in molecular regions containing two bonds or less. This perturbation term accounts for the differences between any two NPs, and it depends also on the exposure times. In convergence with $DD\mu_1(ATO)b_t$, the perturbation term $DD\mu_3(VAN)t_a$ considers the difference between any two NPs, and the exposure times. In this sense, $DD\mu_3(VAN)t_a$ (the third most important descriptor) is associated to the increment in the van der Waals radii of the atoms that form the molecular structures of the NPs in regions having three bonds or less, which will cause a diminution of their toxic effects. We need to point out that $DD\mu_2(ATO)t_a$ and $DD\mu_3(VAN)t_a$ are clear evidences that the toxicities of the NPs are time-dependent. Finally, the descriptor $DD\mu_3(POL)n_s$ involves the changes between any pair of NPs by considering the polarizability in those regions that have three bonds or less, depending also on the shapes of the NPs. Despite its steric nature associated to the molar volume, $DD\mu_3(POL)n_s$ has also electronic information. Thus, the increment of $DD\mu_3(POL)n_s$ means that the higher the polarizability of the metallic atoms accompanying electronegative atoms (O, S, etc) the higher will be the value of this perturbation term, and the lower will be the toxicity of the NPs. However, $DD\mu_3(POL)n_s$ is the least significant descriptor. Therefore, we can envisage the fact that

Table 4. Results obtained from the consensus predictions using the QSTR-perturbation model.

NP	m_e	b_t[a]	n_s[b]	d_m[c]	t_a	s_c[d]	$TE_i(c_j)_{\_nw}$[e]	%CCT[f]
Ag-43.4 nm	CC_{50} (μM)	RAW 264.7 (M)	spherical	H_2O	4	PDADMAC	−1	100.00
Ag-62.6 nm	CC_{50} (μM)	RAW 264.7 (M)	spherical	H_2O	4	UC	−1	85.77
Ag-46.3 nm	CC_{50} (μM)	RAW 264.7 (M)	spherical	H_2O	4	oleate	−1	91.54
Ag-4.5 nm	CC_{50} (μM)	RAW 264.7 (M)	spherical	Dry	4	PDADMAC	−1	100.00
Ag-9 nm	CC_{50} (μM)	RAW 264.7 (M)	spherical	Dry	4	UC	−1	90.77
Ag-4 nm	CC_{50} (μM)	RAW 264.7 (M)	spherical	Dry	4	oleate	−1	90.00
$NiFe_2O_4$-97 nm	CC_{50} (μM)	A549 (H)	irregular	DMEM	24	UC	1	95.77
Fe_2O_3-30 nm (1)	LC_{50} (μM)	*Danio rerio* (embryos)	N/A	Dry	24	UC	1	97.69
Fe_2O_3-30 nm (2)	LC_{50} (μM)	*Danio rerio* (embryos)	N/A	Dry	48	UC	1	97.69
Fe_2O_3-30 nm (3)	LC_{50} (μM)	*Danio rerio* (embryos)	N/A	Dry	72	UC	1	95.38
Fe_2O_3-30 nm (4)	LC_{50} (μM)	*Danio rerio* (embryos)	N/A	Dry	96	UC	1	98.08
Fe_2O_3-30 nm (5)	LC_{50} (μM)	*Danio rerio* (embryos)	N/A	Dry	120	UC	1	98.46
Fe_2O_3-30 nm (6)	LC_{50} (μM)	*Danio rerio* (embryos)	N/A	Dry	168	UC	1	98.08
Ag-34 nm	EC_{50} (μM)	*Pseudokirchneriella subcapitata*	spherical	Dry	72	UC	−1	91.54
Pt-51 nm	EC_{50} (μM)	*Pseudokirchneriella subcapitata*	polyhedral	Dry	72	UC	−1	72.31

[a](M): referred to mouse; (H): referred to human.
[b]N/A: meaning of not available.
[c]DMEM: Abbreviation for Dulbecco's modified Eagle's medium.
[d]PDADMAC: polydiallyldimethylammonium chloride; UC: uncoated nanoparticle.
[e]Referred to the categorical labels assigned to the NPs by comparing their toxicity values with the corresponding cutoffs.
[f]Consensus percentage, i.e. the percentage of times in which the QSTR-perturbation model could correctly predict the nanoparticle according to its observed value $TE_i(c_j)_{\_nw}$.

the variations of this descriptor should be small. It is important to emphasize here that all the variations in the values of the descriptors/perturbation terms of the type $DD\mu_k(PP)c_j$ are somehow related with the increment of the molar volume, and as explained above, this property may have a strong correlation with the ability of the NPs to undergo agglomeration/aggregation. The variations of the molar volume and its related properties (molecular weight/molar mass and polarizability) explained above are only valid for NPs other than those composed by metals. That is, in the case of the metallic NPs, all such variations can cause opposite toxicity effects.

The presence of organic molecules in the surface of the NPs (coating agents) is one of the most important factors that has influence in the toxicity of the NPs. For instance, for diminishing the toxic effects of the NPs, it is necessary to decrease the hydrophobicity of the coating agents in molecular regions formed by two bonds or less. This information is embodied in $DG\mu_2(HYD)$, which considers the differences in the chemical structures between the coating agents present in any two NPs used in the reference and new (output) states. This decline in the hydrophobicity goes along with the augmentation of the polar surface area in those molecular regions containing five bonds or less (five-membered rings included). That information is described by $DG\mu_5(PSA)$ due to its dependence on the difference of the chemical structures between the coating agents used in any two NPs. Consequently, the larger the polar surface attached to the NPs the lower will be the probability of the NPs to exhibit toxic effects.

Predicting general toxicity profiles of new NPs

Until now, all the statistical analyses indicate that the present QSTR-perturbation model based on ANN is able to integrate multiple kinds of chemical and toxicity data of NPs under many different experimental conditions. In order to confirm the practical applications of the present model, we have decided to predict the toxicity of diverse types of NPs formed by silver (Ag), nickel ferrite ($NiFe_2O_4$), iron(III) oxide (Fe_2O_3), and platinum (Pt). These new NPs were not employed in any of the sets involved in the construction of our original dataset (training and validation sets). In fact, they were collected from diverse external sources found in the literature (Ahamed et al. 2011; Ksiazyk et al. 2015; Suresh et al. 2012; Zhu et al. 2012). All the experimental data, as well as the results of the predictions can be found in SI (file SM8), while a summary is depicted in Table 4.

Here, it should be pointed out that the decision of predicting a NP to belong to a specific group or class (nontoxic and toxic) was based on consensus predictions. In this context, the QSTR-perturbation model based on ANN was used to predict each new NP 260 times, that is exactly the same number of

NPs of our original dataset. For accomplishing this task, we defined a statistical index called consensus percentage (%CCT). This is the percentage of times in which a NP is correctly classified/predicted in a given experimental condition according to its observed group/class of $TE_i(c_j)\_nw$ (assigned from the comparison between the experimental value of toxicity and its corresponding cutoff). If %CCT > 50%, the NP is considered as correctly predicted. If %CCT < 50%, the NP is considered as incorrectly predicted. As when %CCT = 50%, it means that the QSTR-perturbation model is leading to a random prediction.

The first case of study was devoted to predict the cytotoxicity of three different Ag-NPs taking into account the fact that they had difference sizes as dry powders, *i.e.* 4.5, 9, and 4 nm (Suresh et al. 2012). The sizes have also been measured in aqueous medium, yielding the respective values of 43.4, 62.6, and 46.3 nm. Additionally, two coating agents have been used, namely: polydiallyldimethylammonium chloride (PDADMAC) and oleate. In any case, the highest value of cytotoxicity determined for these spherical Ag-NPs against RAW 264.7 mouse cells was 4.9 mg/L [equivalent to CC50 (μM) = 45.426], for an exposure time equal to 4 h. Thus, if we compare this value with the corresponding cutoff associated to CC_{50} (μM), it is evident that all the Ag-NPs should be predicted as toxic. For this reason, our purpose here was to demonstrate that regardless of the sizes, the alternative aqueous medium, and the coating agents, Ag-NPs should be toxic against the RAW 264.7 (M) cells. The results of the predictions show that %CCT value is higher than 85%, clearly indicating that all the Ag-NPs are very toxic, and the variations of the different experimental conditions are not enough to change this biological behavior. It should be noticed that there are differences in the %CCT values for the Ag-NPs that use PDADMAC and oleate. The QSTR-perturbation model suggests that even when all the Ag-NPs were correctly predicted as toxic, those coated with oleate seem to have a lower degree of toxicity. This aspect can be explained because oleate has a larger polar surface area [higher value of $DG\mu_5(PSA)$] than PDADMAC, which helps to decrease the toxic effect.

The second case of study was focused on the prediction of the cytotoxicity of uncoated $NiFe_2O_4$-NPs with a size of 97 nm measured in DMEM (Dulbecco's modified Eagle's medium) (Ahamed et al. 2011). These NPs with irregular shape have been assayed against A549 human cells, during a period of 24 hrs. The data in Table 4 indicate that the magnitude of the cytotoxicity is higher than 100 μg/mL (CC_{50} (μM) > 426.652 μM). Because of this large value, $NiFe_2O_4$-NPs should be predicted as nontoxic. The results of our predictions strongly converge with this assumption, confirming the experimental tests. Indeed, $NiFe_2O_4$-NPs were predicted as nontoxic in 95.77% of the times.

A third case of study was focused on predicting the ecotoxic effect of uncoated Fe_2O_3-NPs (shape was not available) against *Danio rerio* (embryos) (Zhu et al. 2012). The LC_{50} value reported for these NPs was 53.35 mg/L [LC_{50} (μM) = 334.08], and it was measured for a period of 168 hrs. The authors of this research also tested the Fe_2O_3-NPs over other exposure times, demonstrating that the toxic effects were time-dependent. According to the LC_{50} value, one should expect that the Fe_2O_3-NPs are to be classified as nontoxic by the QSTR-perturbation model based on ANN. Notice that if the toxicity of these NPs is time-dependent, then, the LC_{50} (μM) ≥ 334.08 for shorter exposure times. Thus, in an attempt to provide a complete virtual screening of the Fe_2O_3-NPs, we have predicted them over six different exposure times (24, 48, 72, 96, 120, and 168 h), all of them considered in the experimental report (Zhu et al. 2012). As can be seen in Table 4, the %CCT values are higher than 95%. The theoretical results are thus in great agreement with the ecotoxicity assays.

The last case of study involved the use of two different types of uncoated NPs formed by the elements Ag and Pt with sizes 34 and 51 nm, respectively (Ksiazyk et al. 2015). Both NPs were tested against the microalga *Pseudokirchneriella subcapitata* for an exposure time of 72 h. From one side, the spherical Ag-NPs exhibited an effective inhibitory concentration of 1.63 mg/L [EC_{50} (μM) = 15.11]. On the other hand, the value of the same measure of ecotoxicity for the polyhedral Pt-NPs was 16.9 mg/L [EC_{50} (μM) = 86.63]. In both cases, the values of the ecotoxic effects and their comparisons with the corresponding cutoff suggest that these two types of NPs are toxic. Our predictions revealed the veracity of this assumption. This is, Ag-NPs were predicted as toxic in 91.54% of the times, while in 72.31% for the Pt-NPs. Even when these two types of NPs were

correctly predicted as toxic by the QSTR-perturbation ANN-based model, the difference in the %CCT values can be explained in terms of their size and chemical composition. For instance, Pt-NPs have larger size, and as commented above, that will definitely play a role in diminishing toxic effects. At the same time, Pt is more electronegative than Ag, meaning that its higher electronegativity will prevent in more degree the release of ions, which constitutes one of the principal mechanisms of toxicity of the metallic NPs, lethal to the biological systems.

Conclusions

Over the past few decades, nanotechnology has infiltrated deeply into human's everyday life. This stems from the recent growing number of applications of nanoparticles in optics, electronics, and medicine, to name just a few. Concerns over the potential health and environmental consequences of nanomaterials have also upraised in the last decade. The application of computational approaches that do not require testing *per se* is an efficient and cheap alternative for the risk assessment of NPs, contributing to enable their safety uses and manipulations. The QSTR-perturbation ANN-based model proposed here aimed to demonstrate the possibility of such computational attempts. The model was indeed able to correctly classify/predict multiple toxicological behaviors of many diverse NPs under dissimilar sets of assay conditions, with a very good performance. In addition, along with the physicochemical interpretation of its descriptors, and the virtual screening of new NPs, it was possible to provide deeper insights regarding the factors responsible for the appearance and/or enhancement of the toxicity. Overall, it is then expected that the present QSTR model is a promising tool that may aid in the future to establish more precise regulatory guidelines forward-identifying the potential hazard of existing and novel engineered nanomaterials.

Disclosure statement

The authors declare no competing financial interest.

Funding

This work received financial support from Fundação para a Ciência e a Tecnologia (FCT/MEC) through national funds, and co-financed by the European Union (FEDER funds) under the Partnership Agreement PT2020, through projects UID/QUI/50006/2013, POCI/01/0145/FEDER/007265, NORTE-01-0145-FEDER-000011 (LAQV@REQUIMTE), and the Interreg SUDOE NanoDesk (SOE1/P1/E0215; UP). RC acknowledges also FCT and the European Social Fund for financial support (Grant SFRH/BPD/80605/2011). To all financing sources the authors are greatly indebted.

References

Ahamed, M. 2011. "Toxic Response of Nickel Nanoparticles in Human Lung Epithelial A549 Cells." *Toxicology in Vitro: An International Journal Published in Association with Bibra* 25: 930–936.

Ahamed, M., M. J. Akhtar, M. A. Siddiqui, J. Ahmad, J. Musarrat, A. A. Al-Khedhairy, M. S. AlSalhi, and S. A. Alrokayan. 2011. "Oxidative Stress Mediated Apoptosis Induced by Nickel Ferrite Nanoparticles in Cultured A549 Cells." *Toxicology* 283: 101–108.

Ahamed, M., D. Ali, H. A. Alhadlaq, and M. J. Akhtar. 2013. "Nickel Oxide Nanoparticles Exert Cytotoxicity via Oxidative Stress and Induce Apoptotic Response in Human Liver Cells (HepG2)." *Chemosphere* 93: 2514–2522.

Ahamed, M., M. A. Siddiqui, M. J. Akhtar, I. Ahmad, A. B. Pant, and H. A. Alhadlaq. 2010. "Genotoxic Potential of Copper Oxide Nanoparticles in Human Lung Epithelial Cells." *Biochemical and Biophysical Research Communications* 396: 578–583.

Artells, E., J. Issartel, M. Auffan, D. Borschneck, A. Thill, M. Tella, L. Brousset, J. Rose, J. Y. Bottero, and A. Thiery. 2013. "Exposure to Cerium Dioxide Nanoparticles Differently Affect Swimming Performance and Survival in Two Daphnid Species." *PLoS One* 8: e71260.

Asharani, P. V., Y. Lianwu, Z. Gong, and S. Valiyaveettil. 2011. "Comparison of the Toxicity of Silver, Gold and Platinum Nanoparticles in Developing Zebrafish Embryos." *Nanotoxicology* 5: 43–54.

Bar-Ilan, O., R. M. Albrecht, V. E. Fako, and D. Y. Furgeson. 2009. "Toxicity Assessments of Multisized Gold and Silver Nanoparticles in Zebrafish Embryos." *Small* 5: 1897–1910.

Bhattacharjee, S., I. M. Rietjens, M. P. Singh, T. M. Atkins, T. K. Purkait, Z. Xu, S. Regli, et al. 2013. "Cytotoxicity of Surface-Functionalized Silicon and Germanium Nanoparticles: The Dominant Role of Surface Charges." *Nanoscale* 5: 4870–4883.

Biffis, A., and M. Králik. 2001. "Catalysis by Metal Nanoparticles Supported on Functional Organic Polymers." *Journal of Molecular Catalysis A* 177: 113–138.

Brigger, I., C. Dubernet, and P. Couvreur. 2002. "Nanoparticles in Cancer Therapy and Diagnosis." *Advanced Drug Delivery Reviews* 54: 631–651.

Carlson, C.,. S. M. Hussain, A. M. Schrand, L. K. Braydich-Stolle, K. L. Hess, R. L. Jones, and J. J. Schlager. 2008. "Unique Cellular Interaction of Silver Nanoparticles: Size-dependent Generation of Reactive Oxygen Species." *The Journal of Physical Chemistry B* 112: 13608–13619.

Coradeghini, R., S. Gioria, C. P. Garcia, P. Nativo, F. Franchini, D. Gilliland, J. Ponti, and F. Rossi. 2013. "Size-dependent Toxicity and Cell Interaction Mechanisms of Gold Nanoparticles on Mouse Fibroblasts." *Toxicology Letters* 217: 205–216.

Corchero, J. L., and A. Villaverde. 2009. "Biomedical Applications of Distally Controlled Magnetic Nanoparticles." *Trends in Biotechnology* 27: 468–476.

Chan, N. Y., M. Zhao, N. Wang, K. Au, J. Wang, L. W. Chan, and J. Dai. 2013. "Palladium Nanoparticle Enhanced Giant Photoresponse at LaAlO/SrTiO Two-Dimensional Electron Gas Heterostructures." *ACS Nano* 7: 8673–8679.

Chen, C. Y., J. R. Retamal, I. W. Wu, D. H. Lien, M. W. Chen, Y. Ding, Y. L. Chueh, C. I. Wu, and J. H. He. 2012. "Probing Surface Band Bending of Surface-engineered Metal Oxide Nanowires." *ACS Nano* 6: 9366–9372.

Chen, P. J., W. L. Wu, and K. C. Wu. 2013. "The Zerovalent Iron Nanoparticle Causes Higher Developmental Toxicity than its Oxidation Products in Early Life Stages of Medaka Fish." *Water Research* 47: 3899–3909.

Cho, J. G., K. T. Kim, T. K. Ryu, J. W. Lee, J. E. Kim, J. Kim, B. C. Lee, et al. 2013. "Stepwise Embryonic Toxicity of Silver Nanoparticles on *Oryzias latipes*." *Biomedical Research International* 2013: 494671.

Chueh, P. J., R. Y. Liang, Y. H. Lee, Z. M. Zeng, and S. M. Chuang. 2014. "Differential Cytotoxic Effects of Gold Nanoparticles in Different Mammalian Cell Lines." *Journal of Hazardous Materials* 264: 303–312.

Chusuei, C. C., C. H. Wu, S. Mallavarapu, F. Y. Hou, C. M. Hsu, J. G. Winiarz, R. S. Aronstam, and Y. W. Huang. 2013. "Cytotoxicity in the Age of Nano: The Role of Fourth Period Transition Metal Oxide Nanoparticle Physicochemical Properties." *Chemico-Biological Interactions* 206: 319–326.

Epa, V. C., F. R. Burden, C. Tassa, R. Weissleder, S. Shaw, and D. A. Winkler. 2012. "Modeling Biological Activities of Nanoparticles." *Nano Letters* 12: 5808–5812.

Estrada, E., and Y. Gutiérrez. 2002–2004. MODESLAB. v1.5. Santiago de Compostela.

Fourches, D., D. Pu, C. Tassa, R. Weissleder, S. Y. Shaw, R. J. Mumper, and A. Tropsha. 2010. "Quantitative Nanostructure-Activity Relationship Modeling." *ACS Nano* 4: 5703–5712.

Fraga, S., H. Faria, M. E. Soares, J. A. Duarte, L. Soares, E. Pereira, C. Costa-Pereira, J. P. Teixeira, M. de Lourdes Bastos, and H. Carmo. 2013. "Influence of the Surface Coating on the Cytotoxicity, Genotoxicity and Uptake of Gold Nanoparticles in Human HepG2 Cells." *Journal of Applied Toxicology*33: 1111–1119.

Franklin, N. M., N. J. Rogers, S. C. Apte, G. E. Batley, G. E. Gadd, and P. S. Casey. 2007. "Comparative Toxicity of Nanoparticulate ZnO, Bulk ZnO, and $ZnCl_2$ to a Freshwater Microalga (*Pseudokirchneriella subcapitata*): The Importance of Particle Solubility." *Environmental Science & Technology* 41: 8484–8490.

García, A., R. Espinosa, L. Delgado, E. Casals, E. González, V. Puntes, C. Barata, X. Font, and A. Sánchez. 2011. "Acute Toxicity of Cerium Oxide, Titanium Oxide and Iron Oxide Nanoparticles Using Standardized Tests." *Desalination* 269: 136–141.

Gong, N., K. Shao, W. Feng, Z. Lin, C. Liang, and Y. Sun. 2011. "Biotoxicity of Nickel Oxide Nanoparticles and Bio-remediation by Microalgae *Chlorella vulgaris*." *Chemosphere* 83: 510–516.

Gonzalez-Diaz, H., S. Arrasate, A. Gomez-SanJuan, N. Sotomayor, E. Lete, L. Besada-Porto, and J. M. Ruso. 2013. "General Theory for Multiple Input-output Perturbations in Complex Molecular Systems. 1. Linear QSPR Electronegativity Models in Physical, Organic, and Medicinal Chemistry." *Current Topics in Medicinal Chemistry* 13: 1713–1741.

González-Díaz, H., A. Pérez-Bello, M. Cruz-Monteagudo, Y. González-Díaz, L. Santana, and E. Uriarte. 2007. "Chemometrics for QSAR with Low Sequence Homology: Mycobacterial Promoter Sequences Recognition with 2D-RNA Entropies." *Chemometrics and Intelligent Laboratory Systems* 85: 20–26.

Gonzalez, L., L. C. Thomassen, G. Plas, V. Rabolli, D. Napierska, I. Decordier, M. Roelants, et al. 2010. "Exploring the Aneugenic and Clastogenic Potential in the Nanosize Range: A549 Human Lung Carcinoma Cells and Amorphous Monodisperse Silica Nanoparticles as Models." *Nanotoxicology* 4: 382–395.

Griffitt, R. J., J. Luo, J. Gao, J. C. Bonzongo, and D. S. Barber. 2008. "Effects of Particle Composition and Species on Toxicity of Metallic Nanomaterials in Aquatic Organisms." *Environmental Toxicology and Chemistry* 27: 1972–1978.

Grosse, S., L. Evje, and T. Syversen. 2013. "Silver Nanoparticle-induced Cytotoxicity in Rat Brain Endothelial Cell Culture." *Toxicology in Vitro: An International Journal Published in Association with Bibra* 27: 305–313.

Ha, S. W., J. A. Sikorski, M. N. Weitzmann, and G. R. Beck. Jr. 2014. "Bio-active Engineered 50 nm Silica Nanoparticles with Bone Anabolic Activity: Therapeutic Index, Effective Concentration, and Cytotoxicity Profile In Vitro." *Toxicology in Vitro: An International Journal Published in Association with Bibra* 28: 354–364.

Han, X., L. Lai, F. Tian, F. L. Jiang, Q. Xiao, Y. Li, Q. Yu, et al. 2012. "Toxicity of CdTe Quantum Dots on Yeast *Saccharomyces cerevisiae*." *Small* 8: 2680–2689.

Hanczar, B., J. Hua, C. Sima, J. Weinstein, M. Bittner, and E. R. Dougherty. 2010. "Small-sample Precision of ROC-related Estimates." *Bioinformatics* 26: 822–830.

Heinlaan, M., A. Ivask, I. Blinova, H. C. Dubourguier, and A. Kahru. 2008. "Toxicity of Nanosized and Bulk ZnO, CuO and TiO_2 to Bacteria *Vibrio fischeri* and Crustaceans *Daphnia magna* and *Thamnocephalus platyurus*." *Chemosphere* 71: 1308–1316.

Hill, T. and P. Lewicki. 2006. *STATISTICS Methods and Applications. A Comprehensive Reference for Science, Industry and Data Mining*. Tulsa: StatSoft.

Holden, P. A., R. M. Nisbet, H. S. Lenihan, R. J. Miller, G. N. Cherr, J. P. Schimel, and J. L. Gardea-Torresdey. 2013. "Ecological Nanotoxicology: Integrating Nanomaterial Hazard Considerations Across the Subcellular, Population,

Community, and Ecosystems Levels." *Accounts of Chemical Research* 46: 813–822.

Horev-Azaria, L., G. Baldi, D. Beno, D. Bonacchi, U. Golla-Schindler, J. C. Kirkpatrick, S. Kolle, et al. 2013. "Predictive Toxicology of Cobalt Ferrite Nanoparticles: Comparative In-vitro Study of Different Cellular Models Using Methods of Knowledge Discovery from Data." *Particle and Fibre Toxicology* 10: 32.

Hsu, D. D. 2013. Chemicool Periodic Table. Available at: http://www.chemicool.com/. Accessed 24 February 2017.

Huang, G. B., and H. A. Babri. 1998. "Upper Bounds on the Number of Hidden Neurons in Feedforward Networks with Arbitrary Bounded Nonlinear Activation Functions." *IEEE Transactions on Neural Networks* 9: 224–229.

Hund-Rinke, K., and M. Simon. 2006. "Ecotoxic Effect of Photocatalytic Active Nanoparticles (TiO_2) on Algae and Daphnids." *Environmental Science and Pollution Research International* 13: 225–232.

Hussain, S. M., K. L. Hess, J. M. Gearhart, K. T. Geiss, and J. J. Schlager. 2005. "In Vitro Toxicity of Nanoparticles in BRL 3A Rat Liver Cells." *Toxicology in Vitro: An International Journal Published in Association with Bibra* 19: 975–983.

Jeng, H. A., and J. Swanson. 2006. "Toxicity of Metal Oxide Nanoparticles in Mammalian Cells." *Journal of Environmental Science and Health. Part A, Toxic/Hazardous Substances & Environmental Engineering* 41: 2699–2711.

Kar, S., A. Gajewicz, T. Puzyn, and K. Roy. 2014. "Nano-quantitative Structure-Activity Relationship Modeling Using Easily Computable and Interpretable Descriptors for Uptake of Magnetofluorescent Engineered Nanoparticles in Pancreatic Cancer Cells." *Toxicology in Vitro: An International Journal Published in Association with Bibra* 28: 600–606.

Kasemets, K., A. Ivask, H. C. Dubourguier, and A. Kahru. 2009. "Toxicity of Nanoparticles of ZnO, CuO and TiO_2 to Yeast *Saccharomyces cerevisiae*." *Toxicology in Vitro: An International Journal Published in Association with Bibra* 23: 1116–1122.

Kim, B. J., Y. Ko, J. H. Cho, and J. Cho. 2013. "Organic Field-Effect Transistor Memory Devices Using Discrete Ferritin Nanoparticle-Based Gate Dielectrics." *Small* 9: 3784–3791.

Kleandrova, V. V., F. Luan, H. Gonzalez-Diaz, J. M. Ruso, A. Melo, A. Speck-Planche, and M. N. D. S. Cordeiro. 2014a. "Computational Ecotoxicology: Simultaneous Prediction of Ecotoxic Effects of Nanoparticles Under Different Experimental Conditions." *Environment International* 73C: 288–294.

Kleandrova, V. V., F. Luan, H. Gonzalez-Diaz, J. M. Ruso, A. Speck-Planche, and M. N. D. S. Cordeiro. 2014b. "Computational Tool for Risk Assessment of Nanomaterials: Novel QSTR-perturbation Model for Simultaneous Prediction of Ecotoxicity and Cytotoxicity of Uncoated and Coated Nanoparticles Under Multiple Experimental Conditions." *Environmental Science & Technology* 48: 14686–14694.

Ksiazyk, M., M. Asztemborska, R. Steborowski, and G. Bystrzejewska-Piotrowska. 2015. "Toxic Effect of Silver and Platinum Nanoparticles Toward the Freshwater Microalga *Pseudokirchneriella subcapitata*." *Bulletin of Environmental Contamination and Toxicology* 94: 554–558.

Kwon, D., J. Park, S. Y. Choi, and T. H. Yoon. 2014. "Effects of Surface-modifying Ligands on the Colloidal Stability of ZnO Nanoparticle Dispersions in In Vitro Cytotoxicity Test Media." *International Journal of Nanomedicine* 9 Suppl 2: 57–65.

Li, C. H., C. C. Shen, Y. W. Cheng, S. H. Huang, C. C. Wu, C. C. Kao, J. W. Liao, and J. J. Kang. 2012. "Organ Biodistribution, Clearance, and Genotoxicity of Orally Administered Zinc Oxide Nanoparticles in Mice." *Nanotoxicology* 6: 746–756.

Liang, H., C. Jin, Y. Tang, F. Wang, C. Ma, and Y. Yang. 2014. "Cytotoxicity of Silica Nanoparticles on HaCaT Cells." *Journal of Applied Toxicology*34: 367–372.

Liao, L.,. J. Liu, E. C. Dreaden, S. W. Morton, K. E. Shopsowitz, P. T. Hammond, and J. A. Johnson. 2014. "A Convergent Synthetic Platform for Single-nanoparticle Combination Cancer Therapy: Ratiometric Loading and Controlled Release of Cisplatin, Doxorubicin, and Camptothecin." *Journal of the American Chemical Society* 136: 5896–5899.

Lin, D., and B. Xing. 2007. "Phytotoxicity of Nanoparticles: Inhibition of Seed Germination and Root Growth." *Environmental Pollution* 150: 243–250.

Lin, W., Y. W. Huang, X. D. Zhou, and Y. Ma. 2006. "In Vitro Toxicity of Silica Nanoparticles in Human Lung Cancer Cells." *Toxicology and Applied Pharmacology* 217: 252–259.

Liu, R., R. Rallo, S. George, Z. Ji, S. Nair, A. E. Nel, and Y. Cohen. 2011. "Classification NanoSAR Development for Cytotoxicity of Metal Oxide Nanoparticles." *Small* 7: 1118–1126.

Liu, R., R. Rallo, R. Weissleder, C. Tassa, S. Shaw, and Y. Cohen. 2013. "Nano-SAR Development for Bioactivity of Nanoparticles with Considerations of Decision Boundaries." *Small* 9: 1842–1852.

Liz-Marzán, L. M., and Kamat, P. V., eds. 2004. Nanoscale Materials. New York, Boston, Dordrecht, London, Moscow: Kluwer Academic Publishers.

Lu, C. H., B. Willner, and I. Willner. 2013a. "DNA Nanotechnology: From Sensing and DNA Machines to Drug-Delivery Systems." *ACS Nano* 7: 8320–8332.

Lu, P., C. T. Campbell, and Y. Xia. 2013b. "A Sinter-resistant Catalytic System Fabricated by Maneuvering the Selectivity of SiO_2 Deposition onto TiO_2 Surface versus Pt Nanoparticle Surface." *Nano Letters* 13: 4957–4962.

Luan, F., V. V. Kleandrova, H. Gonzalez-Diaz, J. M. Ruso, A. Melo, A. Speck-Planche, and M. N. D. S. Cordeiro. 2014. "Computer-aided Nanotoxicology: Assessing Cytotoxicity of Nanoparticles Under Diverse Experimental Conditions by Using a Novel QSTR-perturbation Approach." *Nanoscale* 6: 10623–10630.

Ma, Y., X. He, P. Zhang, Z. Zhang, Z. Guo, R. Tai, Z. Xu, et al. 2011. "Phytotoxicity and Biotransformation of La_2O_3 Nanoparticles in a Terrestrial Plant Cucumber (*Cucumis sativus*)." *Nanotoxicology* 5: 743–753.

Ma, Y., L. Kuang, X. He, W. Bai, Y. Ding, Z. Zhang, Y. Zhao, and Z. Chai. 2010. "Effects of Rare Earth Oxide Nanoparticles on Root Elongation of Plants." *Chemosphere* 78: 273–279.

Marsalek, B., D. Jancula, E. Marsalkova, M. Mashlan, K. Safarova, J. Tucek, and R. Zboril. 2012. "Multimodal Action and Selective Toxicity of Zerovalent Iron Nanoparticles Against Cyanobacteria." *Environmental Science & Technology* 46: 2316–2323.

Mortimer, M.,. K. Kasemets, and A. Kahru. 2010. "Toxicity of ZnO and CuO Nanoparticles to Ciliated Protozoa *Tetrahymena thermophila*." *Toxicology* 269: 182–189.

Moseler, M.,. M. Walter, B. Yoon, U. Landman, V. Habibpour, C. Harding, S. Kunz, and U. Heiz. 2012. "Oxidation State and Symmetry of Magnesia-supported Pd13O(x) Nanocatalysts Influence Activation Barriers of CO Oxidation." *Journal of the American Chemical Society* 134: 7690–7699.

Motskin, M.,. D. M. Wright, K. Muller, N. Kyle, T. G. Gard, A. E. Porter, and J. N. Skepper. 2009. "Hydroxyapatite Nano and Microparticles: Correlation of Particle Properties with Cytotoxicity and Biostability." *Biomaterials* 30: 3307–3317.

Nations, S., M. Wages, J. E. Canas, J. Maul, C. Theodorakis, and G. P. Cobb. 2011. "Acute Effects of Fe(2) O(3), TiO(2), ZnO and CuO Nanomaterials on *Xenopus laevis*." *Chemosphere* 83: 1053–1061.

Pakrashi, S., S. Dalai, A. Humayun, S. Chakravarty, N. Chandrasekaran, and A. Mukherjee. 2013. "*Ceriodaphnia dubia* as a Potential Bio-Indicator for Assessing Acute Aluminum Oxide Nanoparticle Toxicity in Fresh Water Environment." *PLoS One* 8: e74003.

Puzyn, T., B. Rasulev, A. Gajewicz, X. Hu, T. P. Dasari, A. Michalkova, H. M. Hwang, A. Toropov, D. Leszczynska, and J. Leszczynski. 2011. "Using Nano-QSAR to Predict the Cytotoxicity of Metal Oxide Nanoparticles." *Nature Nanotechnology* 6: 175–178.

Radziun, E., J. Dudkiewicz Wilczynska, I. Ksiazek, K. Nowak, E. L. Anuszewska, A. Kunicki, A. Olszyna, and T. Zabkowski. 2011. "Assessment of the Cytotoxicity of Aluminium Oxide Nanoparticles on Selected Mammalian Cells." *Toxicology in Vitro : An International Journal Published in Association with Bibra* 25: 1694–1700.

Rücker, C., G. Rücker, and M. Meringer. 2007. "Y-Randomization and its Variants in QSPR/QSAR." *Journal of Chemical Information and Modeling* 47: 2345–2357.

Sabbioni, E., S. Fortaner, M. Farina, R. Del Torchio, I. Olivato, C. Petrarca, G. Bernardini, et al. 2014. "Cytotoxicity and Morphological Transforming Potential of Cobalt Nanoparticles, Microparticles and Ions in Balb/3T3 Mouse Fibroblasts: an In Vitro Model." *Nanotoxicology* 8: 455–464.

Sadeghi, L., F. Tanwir, and V. Yousefi Babadi. 2015. "In Vitro Toxicity of Iron Oxide Nanoparticle: Oxidative Damages on Hep G2 Cells." *Experimental and Toxicologic Pathology* 67: 197–203.

Sadiq, I. M., S. Dalai, N. Chandrasekaran, and A. Mukherjee. 2011a. "Ecotoxicity Study of Titania (TiO(2)) NPs on Two Microalgae Species: *Scenedesmus* sp. and *Chlorella* sp." *Ecotoxicology and Environmental Safety* 74: 1180–1187.

Sadiq, I. M., S. Pakrashi, N. Chandrasekaran, and A. Mukherjee. 2011b. "Studies on Toxicity of Aluminum Oxide (Al_2O_3) Nanoparticles to Microalgae Species: *Scenedesmus sp.* and *Chlorella sp*." *Journal of Nanoparticle Research* 13: 3287–3299.

Salunkhe, A. B., V. M. Khot, N. D. Thorat, M. R. Phadatare, C. I. Sathish, D. S. Dhawale, and S. H. Pawar. 2013. "Polyvinyl Alcohol Functionalized Cobalt Ferrite Nanoparticles for Biomedical Applications." *Applied Surface Science* 264: 598–604.

Saquib, Q., A. A. Al-Khedhairy, J. Ahmad, M. A. Siddiqui, S. Dwivedi, S. T. Khan, and J. Musarrat. 2013. "Zinc Ferrite Nanoparticles Activate IL-1b, NFKB1, CCL21 and NOS2 Signaling to Induce Mitochondrial Dependent Intrinsic Apoptotic Pathway in WISH Cells." *Toxicology and Applied Pharmacology* 273: 289–297.

Schoen, D. T., T. Coenen, F. J. Garcia de Abajo, M. L. Brongersma, and A. Polman. 2013. "The Planar Parabolic Optical Antenna." *Nano Letters* 13: 188–193.

Selvaraj, V., S. Bodapati, E. Murray, K. M. Rice, N. Winston, T. Shokuhfar, Y. Zhao, and E. Blough. 2014. "Cytotoxicity and Genotoxicity Caused by Yttrium Oxide Nanoparticles in HEK293 Cells." *International Journal of Nanomedicine* 9: 1379–1391.

Shao, C. Y., S. Z. Chen, B. H. Su, Y. J. Tseng, E. X. Esposito, and A. J. Hopfinger. 2013. "Dependence of QSAR Models on the Selection of Trial Descriptor Sets: a Demonstration Using Nanotoxicity Endpoints of Decorated Nanotubes." *Journal of Chemical Information and Modeling* 53: 142–158.

Silva, T., L. R. Pokhrel, B. Dubey, T. M. Tolaymat, K. J. Maier, and X. Liu. 2014. "Particle Size, Surface Charge and Concentration Dependent Ecotoxicity of Three Organo-Coated Silver Nanoparticles: Comparison Between General Linear Model-predicted and Observed Toxicity." *Science of the Total Environment* 468-469: 968–976.

Song, L., M. Connolly, M. L. Fernandez-Cruz, M. G. Vijver, M. Fernandez, E. Conde, G. R. de Snoo, W. J. Peijnenburg, and J. M. Navas. 2014. "Species-specific Toxicity of Copper Nanoparticles Among Mammalian and Piscine Cell Lines." *Nanotoxicology* 8: 383–393.

Song, U., H. Jun, B. Waldman, J. Roh, Y. Kim, J. Yi, and E. J. Lee. 2013. "Functional Analyses of Nanoparticle Toxicity: a Comparative Study of the Effects of TiO_2 and Ag on Tomatoes (*Lycopersicon esculentum*)." *Ecotoxicology and Environmental Safety* 93: 60–67.

Speck-Planche, A., and V. V. Kleandrova. 2012. "QSAR and Molecular Docking Techniques for the Discovery of Potent Monoamine Oxidase B Inhibitors: Computer-aided Generation of New Rasagiline Bioisosteres." *Current Topics in Medicinal Chemistry* 12: 1734–1747.

Stathakis, D. 2009. "How Many Hidden Layers and Nodes?" *International Journal of Remote Sensing* 30: 2133–2147.

Statsoft-Team. 2001. STATISTICA. Data analysis software system. v6.0. Tulsa.

Suresh, A. K., D. A. Pelletier, W. Wang, J. L. Morrell-Falvey, B. Gu, and M. J. Doktycz. 2012. "Cytotoxicity Induced by Engineered Silver Nanocrystallites is Dependent on Surface Coatings and Cell Types." *Langmuir* 28: 2727–2735.

Tarantola, M., A. Pietuch, D. Schneider, J. Rother, E. Sunnick, C. Rosman, S. Pierrat, C. Sonnichsen, J. Wegener, and A. Janshoff. 2011. "Toxicity of Gold-nanoparticles: Synergistic Effects of Shape and Surface Functionalization on Micromotility of Epithelial Cells." *Nanotoxicology* 5: 254–268.

Toropov, A. A., A. P. Toropova, E. Benfenati, G. Gini, T. Puzyn, D. Leszczynska, and J. Leszczynski. 2012. "Novel Application of the CORAL Software to Model Cytotoxicity of Metal Oxide Nanoparticles to Bacteria *Escherichia coli*." *Chemosphere* 89: 1098–1102.

Truong, L., I. S. Moody, D. P. Stankus, J. A. Nason, M. C. Lonergan, and R. L. Tanguay. 2011. "Differential Stability of Lead Sulfide Nanoparticles Influences Biological Responses in Embryonic Zebrafish." *Archives of Toxicology* 85: 787–798.

Tuominen, M., E. Schultz, and M. Sillanpää. 2013. "Toxicity and Stability of Silver Nanoparticles to the Green Alga *Pseudokirchneriella subcapitata* in Boreal Freshwater Samples and Growth Media." *Nanomaterials and the Environment* 1: 48–57.

Uboldi, C., G. Giudetti, F. Broggi, D. Gilliland, J. Ponti, and F. Rossi. 2012. "Amorphous Silica Nanoparticles do not Induce Cytotoxicity, Cell Transformation or Genotoxicity in Balb/3T3 Mouse Fibroblasts." *Mutation Research* 745: 11–20.

Wang, H., R. L. Wick, and B. Xing. 2009. "Toxicity of Nanoparticulate and Bulk ZnO, Al_2O_3 and TiO_2 to the Nematode *Caenorhabditis elegans*." *Environmental Pollution* 157: 1171–1177.

Wang, Z., N. Li, J. Zhao, J. C. White, P. Qu, and B. Xing. 2012. "CuO Nanoparticle Interaction with Human Epithelial Cells: Cellular Uptake, Location, Export, and Genotoxicity." *Chemical Research in Toxicology* 25: 1512–1521.

Xu, Z., C. Liu, J. Wei, and J. Sun. 2012. "Effects of Four Types of Hydroxyapatite Nanoparticles with Different Nanocrystal Morphologies and Sizes on Apoptosis in Rat Osteoblasts." *Journal of Applied Toxicology : Jat* 32: 429–435.

Yang, B., C. Zhao, M. Xiao, F. Wang, C. Li, J. Wang, and J. C. Yu. 2013. "Loading Metal Nanostructures on Cotton Fabrics as Recyclable Catalysts." *Small* 9: 1003–1007.

Yang, X., J. Liu, H. He, L. Zhou, C. Gong, X. Wang, L. Yang, et al. 2010. "SiO_2 Nanoparticles Induce Cytotoxicity and Protein Expression Alteration in HaCaT Cells." *Particle and Fibre Toxicology* 7: 1

Zanette, C., M. Pelin, M. Crosera, G. Adami, M. Bovenzi, F. F. Larese, and C. Florio. 2011. "Silver Nanoparticles Exert a Long-lasting Antiproliferative Effect on Human Keratinocyte HaCaT Cell Line." *Toxicology in Vitro : An International Journal Published in Association with Bibra* 25: 1053–1060.

Zhang, W., K. Lin, Y. Miao, Q. Dong, C. Huang, H. Wang, M. Guo, and X. Cui. 2012. "Toxicity Assessment of Zebrafish Following Exposure to CdTe QDs." *Journal of Hazardous Materials* 213-214: 413–420.

Zhang, Z.,. J. Wang, and C. Chen. 2013. "Near-infrared Light-mediated Nanoplatforms for Cancer Thermo-chemotherapy and Optical Imaging." *Advanced Materials* 25: 3869–3880.

Zhu, X., Y. Chang, and Y. Chen. 2010. "Toxicity and Bioaccumulation of TiO_2 Nanoparticle Aggregates in *Daphnia magna*." *Chemosphere* 78: 209–215.

Zhu, X., S. Tian, and Z. Cai. 2012. "Toxicity Assessment of Iron Oxide Nanoparticles in Zebrafish (*Danio rerio*) Early Life Stages." *PLoS One* 7: e46286.

Zhu, X., L. Zhu, Y. Chen, and S. Tian. 2009. "Acute Toxicities of Six Manufactured Nanomaterial Suspensions to *Daphnia magna*." *Journal of Nanoparticle Research* 11: 67–75.

Zhu, X., L. Zhu, Z. Duan, R. Qi, Y. Li, and Y. Lang. 2008. "Comparative Toxicity of Several Metal Oxide Nanoparticle Aqueous Suspensions to Zebrafish (*Danio rerio*) Early Developmental Stage." *Journal of Environmental Science and Health. Part A, Toxic/hazardous Substances & Environmental Engineering* 43: 278–284.